ADVANCED ELECTRONIC MATERIALS
www.advelectronicmat.de

Spin-Wave Eigenmodes of Dzyaloshinskii Domain Walls

Pablo Borys, Felipe Garcia-Sanchez, Joo-Von Kim, and Robert L. Stamps**

A theory for the spin-wave eigenmodes of a Dzyaloshinskii domain wall is presented. These walls are Néel-type domain walls that can appear in perpendicularly magnetized ultrathin ferromagnets in the presence of a sizeable Dzyaloshinskii–Moriya interaction. The mode frequencies for spin waves propagating perpendicular to the domain wall plane are computed using a continuum approximation. In contrast to Bloch-type walls, it is found that the spin wave potential associated with Dzyaloshinskii domain walls is not reflectionless, which leads to a finite scattering cross-section for interactions between spin waves and domain walls. A gap produced by the Dzyaloshinskii interaction emerges and band structures arising from periodic wall arrays are discussed.

1. Introduction

The Dzyaloshinskii–Moriya interaction (DMI) is an antisymmetric contribution to the exchange energy that can exist in spin systems that lack inversion symmetry.[1–3] Spin textures stabilized by DMI are of special interest due to the possibility of new technological applications.[4–6] For room temperature operation, interface DMI is of particular importance in terms of thin film structures based on transition metals, compatible with traditional spintronic devices. It has been shown in perpendicular materials that because of DMI compensation of the dipole–dipole interaction at the center of a domain wall, a Néel-type domain wall is favored with important enhancements of domain wall stability and mobility.[7,8] Small amplitude fluctuations of the magnetization about equilibrium—spin waves—in systems with DMI have been studied experimentally,[9] and theoretically[10–12] for interface DMI films. A key feature is nonreciprocity of frequency as a function of propagation direction for finite wavelength spin waves, which emerges from the chiral symmetry breaking DMI. For domain walls, it has been shown that the nonreciprocity appears when spin waves propagate parallel to the domain wall plane.[13,14] In the present work, we focused on spin wave propagation perpendicular to the plane of a DMI-stabilized Néel wall. We found an extra chiral term associated with the DMI in the effective potential that describes the wall and treat it as a perturbation. While the spin waves exhibit a reciprocal dispersion, other interesting features as spin wave reflection by the wall and hybridization of the modes result from the DMI term.

We illustrate the hybridization of the modes and the reflection by considering a magnonic crystal formed by a periodic array of domain walls in a nanowire with DMI. Without DMI, the walls are Bloch-type walls, which are known to represent reflectionless potentials for spin waves traveling through them.[15–17] This results in a gapless band structure. However, with DMI the stable configuration becomes an array of Néel-type walls with a modified potential for the spin waves, which is no longer reflectionless and standing waves appear at the edges of the first Brillouin zone producing gaps in the band structure. This article is organized as follows. In Section 2, the model and calculations involving the static domain wall profile are presented. In Section 3, the spin-wave eigenmodes of the Dzyaloshinskii domain wall are computed using a variational method in the continuum approximation. Consequences of these eigenmodes are then explored in Section 4, where the reflection and transmission coefficients for propagating spin waves through the domain wall are computed and band gaps in associated with periodic wall arrays are discussed. Finally, a discussion and some concluding remarks are given in Section 5.

2. Model and Static Wall Profile

An ultrathin ferromagnetic wire is considered in which a domain wall separates two uniformly magnetized domains along the x axis, as shown in **Figure 1**. For the main purpose of this work, it is more convenient to work with the magnetization as a field $\boldsymbol{M}(\boldsymbol{r})$ rather than with the individual spins. This macroscopic theory remains valid in the long wavelength approximation, $ka \ll 1$, where k and a are the spin-wave vector and the lattice parameter, respectively. It has the advantage that we can easily introduce phenomenological constants related to interface anisotropies, magnetostatic energy, and exchange interaction.

The energies we have considered account for the most important symmetries of the problem, and the magnetization orientation, represented by the unit vector $\boldsymbol{m}$, is parametrized using spherical coordinates as $\boldsymbol{m} = \boldsymbol{M}/|M_s| = (\sin\theta\cos\phi, \sin\theta\sin\phi, \cos\theta)$, where $\theta = \theta(\boldsymbol{r}, t)$, $\phi = \phi(\boldsymbol{r}, t)$ and M_s is the saturation

P. Borys, Prof. R. L. Stamps
SUPA
School of Physics and Astronomy
University of Glasgow
Glasgow G12 8QQ, UK
p.borys-sosa.1@research.gla.ac.uk;
Robert.Stamps@glasgow.ac.uk
Dr. F. Garcia-Sanchez, Dr. J.-V. Kim
Institut d'Electronique Fondmentale
CNRS, Univ. Paris-Sud
Université Paris-Saclay
91405, Orsay, France

DOI: 10.1002/aelm.201500202

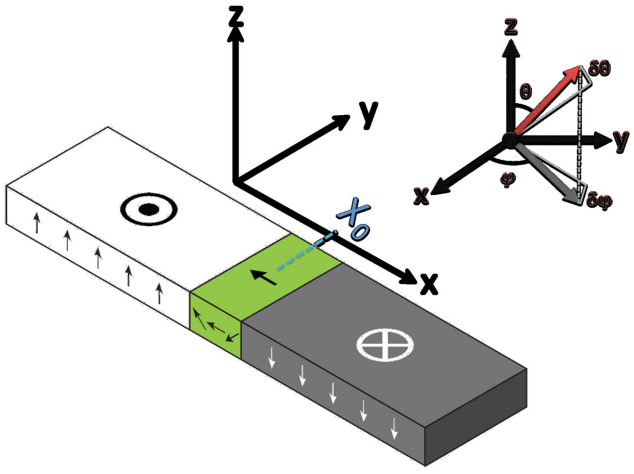

Figure 1. Geometry considered for the Néel-type Dzyaloshinskii domain wall. X_0 denotes the position of the wall center along the x axis. Translational invariance is assumed along the y-direction and the magnetization is taken to be uniform across the thickness of the film in the z-direction. Small fluctuations ($\delta\theta$, $\delta\phi$) are presented when the magnetization is parametrized in spherical coordinate.

magnetization. The total magnetic energy of this system is given by the functional $U[\theta(\boldsymbol{r}), \phi(\boldsymbol{r})]$,

$$U = \int \mathrm{d}V \Big[A\left((\nabla\theta)^2 + \sin^2\theta(\nabla\phi)^2\right) + D\left(\frac{\partial\theta}{\partial x}\cos\phi + \frac{\partial\theta}{\partial y}\sin\phi + \frac{1}{2}\sin 2\theta\left(\frac{\partial\phi}{\partial y}\cos\phi - \frac{\partial\phi}{\partial x}\sin\phi\right)\right) + \left(K_\mathrm{u} + K_\perp\cos^2\phi\right)\sin^2\theta\Big]. \quad (1)$$

The first term describes the isotropic part of the exchange interaction and where the exchange stiffness constant A is related within the continuum approximation to the exchange integral J in a simple cubic lattice by $A = JS^2/a$, with a is the lattice constant and S is the spin. The second term describes the antisymmetric contribution to the exchange interaction given by the DMI. Unlike the isotropic part, this interaction is linear in the spatial derivatives of the magnetization. For a multilayer system with a heavy-metal substrate its from is given in terms of the Lifshitz invariants $L_{ij}^k = m_i\frac{\partial m_j}{\partial x_k} - m_j\frac{\partial m_i}{\partial x_k}$ as $D\left(L_{zx}^x + L_{zy}^y\right)$.[7,18]

Finally, the third term describes the total anisotropy of the system. The constant $K_\mathrm{o} = K_\mathrm{u} - \mu_0 M_\mathrm{s}^2/2$ is the effective anisotropy along the z axis, where K_u is related to the magnetocrystalline anisotropy and $-\mu_0 M_\mathrm{s}^2/2$ accounts for the perpendicular demagnetizing field effect in the local approximation. The constant $K_\perp$, that favors a Bloch-over a Néel-type wall in the absence of DMI, is a magnetostatic anisotropy along the x axis related to the demagnetizing coefficient N_x by $K_\perp = \mu_0 N_x M_\mathrm{s}^2/2$ in the local approximation.

The static profile of the domain wall is determined by minimizing the energy functional in Equation (1) with respect to (θ_0, ϕ_0). We assume a straight wall so that there is translational invariance along the y-direction. Furthermore, we assume a planar wall, which requires $\phi(x) = \phi_0$. The equations satisfied by the static wall profile (θ_0, ϕ_0) are given by

$$\frac{\delta U}{\delta\theta} = 0 \Rightarrow A\frac{\partial^2\theta_0}{\partial x^2} - \frac{1}{2}\left(K_\mathrm{o} + K_\perp\cos^2(\phi_0)\right)\sin(2\theta_0) = 0, \quad (2)$$

$$\frac{\delta U}{\delta\phi} = 0 \Rightarrow \sin(\phi_0)\sin^2(\theta_0)\left(K_\perp\cos(\phi_0) + D\frac{\partial\theta_0}{\partial x}\right) = 0, \quad (3)$$

which are two coupled, nonlinear differential equations. Note that the second equation above is satisfied by the ϕ_0 ansatz for finite values of the DMI, $D \neq 0$, only if the domain wall assumes a pure Néel profile ($\phi_0 = 0$ or π). By assuming a Néel wall state, the solution for $\theta_0(x)$ can be written as the usual domain wall profile with a width $\lambda = \sqrt{A/(K_\mathrm{u} + K_\perp)}$

$$\theta_0(x) = 2\tan^{-1}\left[\exp\left(\pm\frac{x - X_0}{\lambda}\right)\right], \quad (4)$$

where X_0 denotes the wall center, which is arbitrary. The solution with the positive sign in the argument of the exponential function gives the configuration illustrated in Figure 1. With this solution, the total domain wall energy (1) can be evaluated to be

$$\sigma_\mathrm{w} \equiv U\left[\theta_0, \phi_0\right] = 4\sqrt{A(K_\mathrm{u} + K_\perp)} \mp \pi D, \quad (5)$$

where the negative sign corresponds to the solution $\phi_0 = \pi$ and the positive sign to $\phi_0 = 0$, which indicates that left-handed Néel walls are preferred energetically for $D > D_\mathrm{c} = 4\lambda K_\perp/\pi > 0$.

3. Spin-Wave Hamiltonian

We are interested in linearized excitations about the stable configuration. We approach this by expanding the magnetic energy functional, Equation (1), up to second order in small fluctuations ($\delta\theta$, $\delta\phi$), depicted in Figure 1, around (θ_0, ϕ_0). By allowing the fluctuations to vary in space,[16,19] we can identify the spin-wave Hamiltonian,

$$\delta H = \left(K_\mathrm{o} + K_\perp\right)\int \mathrm{d}V \delta\theta\left[-\lambda^2\partial_x^2 + V_\mathrm{P}(x)\right]\delta\theta + \delta\phi\left[-\lambda^2\partial_x^2 + V_\mathrm{P}(x) + \frac{D}{\lambda\left(K_\mathrm{o} + K_\perp\right)}(x/\lambda) - \frac{K_\perp}{K_\mathrm{o} + K_\perp}\right]\delta\phi, \quad (6)$$

where $V_\mathrm{P}(x) = [1 - 2\,\mathrm{sech}^2(x/\lambda)]$. The physical picture of Equation (6) can be thought of as a wave traveling through an effective potential specified by the underlying domain wall, wherein the hyperbolic secant terms account for the domain wall structure. In particular, the DMI term, $D\,\mathrm{sech}(x/\lambda)$, results from the chiral symmetry breaking of the stable configuration given by a left-handed Néel-type wall. There is an elliptical precession in the fluctuations because of the extra terms in the $\delta\phi$ component due to the DMI and the $K_\perp$.

Interestingly, while the $K_\perp$ produces a constant ellipticity, the DMI introduces a spatial dependent ellipticity through the D sech(x/λ) term. The Schrödinger type operator, $-\lambda^2\partial_x^2 + V_P(x)$, has been widely studied and is used to describe spin waves in a Bloch-type domain wall.[19–22] Solutions to these operator include a single-bond state,

$$\xi_{\rm loc}(x) = \frac{1}{\sqrt{2\lambda}}\,\mathrm{sech}\left(x/\lambda\right) \tag{7}$$

with zero corresponding energy, and continuum-traveling states,

$$\xi_k(x) = \frac{1}{\sqrt{\omega_k}} e^{ikx}[\tanh(x/\lambda) - ik\lambda], \tag{8}$$

with eigenenergy given by $\omega_k = 1 + k^2\lambda^2$. The above states form a complete orthonormal set,

$$\begin{aligned} \int \mathrm{d}V \xi_k^* \xi_{\rm loc} &= 0, \\ \int \mathrm{d}V \xi_k^* \xi_m &= \delta_{k,m}. \end{aligned} \tag{9}$$

with which we can now expand our solutions to include the effects of DMI as a perturbation. We propose a linear superposition of the local and traveling modes,

$$\chi(x) = i\delta\phi(x) + \delta\theta(x) = ic_{\rm loc}\xi_{\rm loc}(x) + \sum\nolimits_k d_k \xi_k(x), \tag{10}$$

to calculate the spin-wave energy. After the space integrals are computed, we find

$$\begin{aligned} \delta H = &-c_{\rm loc}^2\left(\frac{\pi D}{4\lambda} + K_\perp\right) \\ &+ \sum_k \left[A_k' d_k^* d_k + B_k'\left(d_k^* d_{-k}^* + d_k d_{-k}\right) + C_k c_{\rm loc}\left(d_k + d_k^*\right)\right] \\ &+ \sum_{km} U_{km} d_k^* d_m + V_{km}\left(d_k d_m + d_k^* d_m^*\right), \end{aligned} \tag{11}$$

where the coefficients are given by

$$\begin{aligned} A_k' &= \omega_k(K_u + K_\perp) - \frac{K_\perp}{2}, \\ B_k' &= \frac{K_\perp}{4}, \\ C_k &= \int \mathrm{d}V \xi_{\rm loc}\Delta(x)\xi_k, \\ U_{km} &= \int \mathrm{d}V \xi_k^*\Delta(x)\xi_m, \\ V_{km} &= \int \mathrm{d}V\left(\xi_k\Delta(x)\xi_m + \xi_k^*\Delta(x)\xi_m^*\right). \end{aligned} \tag{12}$$

The A'_k and B'_k terms denote elliptical spin precession as a result of the transverse anisotropy described by $K_\perp$ and correspond to the usual terms found in the Bloch wall case.[14,19] The C_k, U_{km}, and V_{km} terms are proportional to the strength of D and depend on k because these terms result from the spatial dependent ellipticity.

The C_k terms represents the coupling between the local and the traveling modes, it is small compared to the other terms so it will not be considered. U_{km} and V_{km} are scattering terms that describe the transition from a state with momentum $\hbar k$ to another state with $\hbar m$. If we focus on the maximum scattering strength then the specific form of the coefficients, $U_{\rm km} \approx \mathrm{sech}(k-m)$ and $V_{km} \approx \mathrm{sech}(k+m)$, allows us to approximate U_{km} and V_{km} by delta functions δ_{km}, δ_{k-m}, respectively. We can then approximate δH as

$$\delta H = -c_{\rm loc}^2\left(\frac{\pi D}{4\lambda} + K_\perp\right) + \sum\nolimits_k A_k d_k^* d_k + B_k\left(d_k^* d_{-k}^* + d_k d_{-k}\right). \tag{13}$$

The first term on the right hand side of Equation (13) can be related to the domain wall mass by $p^2/(2m_N) \approx c_{\rm loc}^2\left(\frac{\pi D}{4\lambda} + K_\perp\right)$, where $m_N = 1/\left[2\left(\frac{\pi D}{4\lambda} + K_\perp\right)\right]$ is the Néel-type domain wall mass.[23,24] The mass in a Bloch-type wall is $m_B = 1/(2K_\perp)$ so $m_{\rm N} < m_{\rm B}$, which agrees with a higher mobility in Dzyaloshinskii domain walls.[25,26] The remaining coefficients are

$$\begin{aligned} A_k &= \omega_k(K_{\rm o} + K_\perp) - \frac{K_\perp}{2} + \frac{\pi D}{4\lambda}\frac{\left(1+2k^2\lambda^2\right)}{\omega_k}, \\ B_k &= \frac{K_\perp}{4} - \frac{\pi D}{8\lambda}\frac{\left(1+2k^2\lambda^2\right)}{\omega_k}. \end{aligned} \tag{14}$$

In the limit $D \to 0$, $K_\perp \to 0$, $B_k = 0$ and the frequency corresponds to that of a uniformly magnetized film, $\Omega_k{}^{\rm u} = 1/\hbar\ (Ak^2 + K_{\rm o})$. Equation (13) can be diagonalized by means of a Bogoliubov transformation, $c_k = u_k^+ d_k - u_k^- d_k^*$, $u_k^\pm = \sqrt{(A_k \pm \hbar\Omega_k)/2\hbar\Omega_k}$, to obtain

$$\delta H = -c_{\rm loc}^2\left(\frac{\pi D}{4\lambda} + K_\perp\right) + \sum\nolimits_k \hbar\Omega_k c_k^* c_k \tag{15}$$

where the frequency Ω_k is given by

$$\Omega_k = \frac{(K_{\rm o} + K_\perp)a^3}{\hbar}\sqrt{\omega_k\left(\omega_k - \frac{K_\perp}{K_{\rm o} + K_\perp} + \frac{\pi D}{4\lambda(K_{\rm o} + K_\perp)}\frac{\left(1+2k^2\lambda^2\right)}{\left(1+k^2\lambda^2\right)}\right)}, \tag{16}$$

where $a \approx 0.3$ nm is the lattice constant. We find a critical value, $D_{c2} = 4\sqrt{AK_{\rm o}}/\pi \approx 3.6\,\mathrm{mJm^{-2}}$, in the limit $k \to 0$ that agrees with previous work,[7,14,27] above which the domain wall becomes unstable. It is common to find a nonreciprocal dispersion in systems under the influence of the DMI, however, this is not the case for the direction of propagation considered here. It has been shown that the nonreciprocity arises for propagation parallel to the plane of the wall,[13,14] which in our geometry corresponds to propagation along the y-direction. Still, an interesting consequence, related with the reflection of the spin waves, can be envisaged when we write the spin waves eigenmodes in terms of the amplitudes c_k, c^*_{-k},

$$\chi(x) = ic_{\rm loc}\xi_{\rm loc}(x) + \sum\nolimits_k \left(c_k u_k^+ + c_{-k}^* u_k^-\right)\xi_k(x) \tag{17}$$

There is a hybridization between the localized mode, $\xi_{\rm loc}(x)$, and the traveling modes, $\xi_k(x)$ resulting from the DMI and $K_\perp$,

which are the terms inducing the ellipticity in the precession. For clarity, we define $\theta_k = c_k + c^*_k$ and $\phi_k = (c_k - c^*_k)/i$, so that the small fluctuations are given by

$$\begin{aligned}\delta\theta(x) &= \sum_k \varepsilon^\theta \theta_k \xi_k(x),\\ \delta\phi(x) &= c_{\rm loc}\xi_{\rm loc}(x) + \sum_k \varepsilon^\phi \phi_k \xi_k(x),\end{aligned} \tag{18}$$

where the parameters $\varepsilon^\theta = (u_k^+ + u_k^-)/2$ and $\varepsilon^\phi = (u_k^+ + u_k^-)/2$ represent the ellipticity in the spin precession. In a totally symmetric system ($K_\perp = 0$, $D = 0$), the spins are circularly polarized, i.e., $\varepsilon^\theta = \varepsilon^\phi = 1/2$.

4. Band Structure in Periodic Wall Arrays

We have discussed the effects of the DMI in the spin-wave dispersion. We now examine how a DMI-driven Néel-type wall scatters the spin waves. The scattering potential for spin waves in a Bloch ($D = 0$) domain wall is represented by $-\lambda^2\partial_x^2 + V_P(x)$, which is reflectionless but leads to a phase shift when spin waves propagate through it.[17,28] This reflectionless potential corresponds to a specific case of the so-called modified Pöschl–Teller Hamiltonian,[20]

$$\left[-\alpha^2\partial_x^2 - l(l-1)\,\mathrm{sech}^2(x/\alpha)\right]\psi = \epsilon\psi. \tag{19}$$

The parameter l describes the depth of the potential well, α has units of distance and ϵ is a dimensionless energy for the wave. For a Bloch-type wall, $l = 2$ and $\alpha = \lambda$. The transmission and reflection coefficients related to the wave propagation across this potential have been calculated for this Hamiltonian as a function of the depth

$$|R|^2 = \frac{1}{1+p^2}; \qquad |T|^2 = \frac{p^2}{1+p^2}, \tag{20}$$

with $p = \sinh(\pi k\alpha)/\sin(\pi l)$.[29] From this result, it can be seen by inspection that for $l \in N$ $|R|^2$ is zero. For the Dzyaloshinskii domain walls, the Hamiltonian is

$$\left[-\lambda^2\partial_x^2 - 2^2(x/\lambda) - \frac{D\,\mathrm{sech}(x/\lambda)}{\lambda(K_u + K_\perp)}\right]\chi(x) = E\chi(x), \tag{21}$$

where the dimensionless energy is $E = \dfrac{\hbar\Omega_k}{(K_u + K_\perp)a^3} + \kappa - 1$. We define the dimensionless parameter $D' = D/(\lambda(K_o + K_\perp))$. It is possible to write Equation (21) as

$$\left[-\lambda^2\partial_x^2 - \left(2 + D'\cosh(x/\lambda)\right)^2(x/\lambda)\right]\chi(x) = E\chi(x), \tag{22}$$

from where we can relate the depth l in Equation (19) with the DMI part in the effective potential,

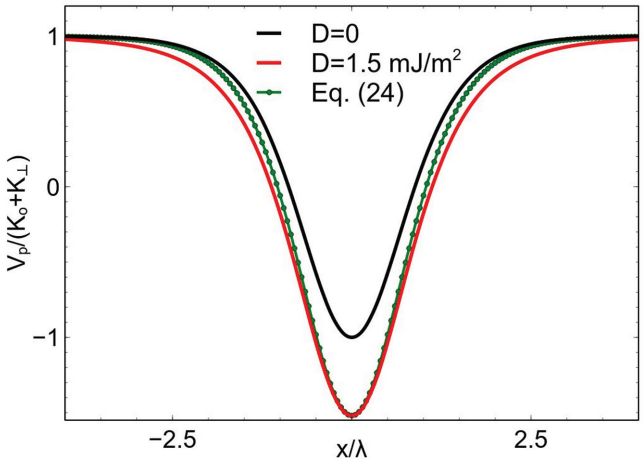

Figure 2. Effective potentials associated with the domain wall. The solid lines represent the exact form of the potentials, in black for a Bloch-type domain wall and in red for a Dzyaloshinskii domain wall with D = 1.5 mJ m^{-2}. The dotted line is the potential calculated using Equation (24).

$$\begin{aligned}&l(l-1) = 2 + D'\cosh x/\lambda\\ &l = \frac{1}{2}\left[1 \pm \sqrt{1 + 4\left(2 + D'\cosh(x/\lambda)\right)}\right]\end{aligned}. \tag{23}$$

The depth l now has a spatial dependence due to the DMI. To make further progress we examine the form of the total effective potential and compare it with the Bloch-type potential, they are shown as solid lines in **Figure 2**. Although there is a small deformation in the total effective potential as compared to the Bloch-type one, the main effect of the DMI is to increase the depth l. As the depth is measured at $x = 0$ we then take $\cosh(x/\lambda) = 1$ in Equation (23). Furthermore, the depth increases due to the DMI so that we take the positive root solution in Equation (23) as the physical solution. Under these assumptions the depth l is given by

$$l = \frac{1}{2}\left[1 + \sqrt{1 + 4\left(2 + \frac{D}{\lambda(K_u + K_\perp)}\right)}\right]. \tag{24}$$

We show the potential obtained using Equation (24) as the dotted curve in Figure 2, it corresponds to the exact form of a modified Pöschl Teller potential. In the domain wall region $-1 < x/\lambda < 1$ no deformation can be observed, the maximum deviation at $x/\lambda = \pm 1$ is less than a tenth of $V_P/(K_o + K_\perp)$. Note that considering the opposite chirality, $D < 0$, results in a decrease of the depth and then the negative root solution in (23) would be the physical solution, and the same considerations apply.

Two transmission coefficients were calculated as a function of the wave vector k using Equation (24) for different values of D and are shown in **Figure 3**. We include numerical simulations to verify that our assumption is reasonable. The numerical calculations were performed within a micromagnetic model. The calculations were done with the code mumax3.[30] The standard code includes the interface DMI term but was modified to include at the same time the effective in-plane and out-of-plane anisotropies. The parameters used were

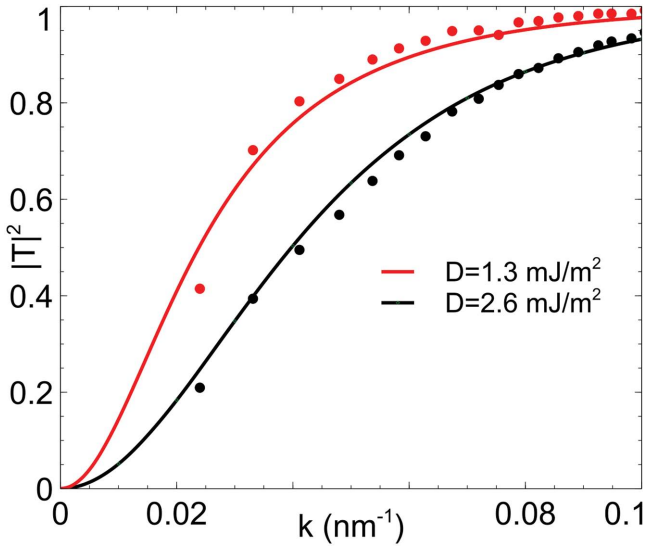

Figure 3. Transmission coefficient for D = 1.3 mJ m^{-2} (red) and D = 2.6 mJ m^{-2} (black). The solid lines result from using equation (22) and the points are numerical simulations as described in the text.

A = 16 pJ m$^{-}K_{\perp}$ = 18 kJ m^{-3}, K_u = 0.5 MJ m^{-3} and λ = 5.55 nm. The system was discretized in cells of 1.5625 × 1.5625 × 1 nm^3. The geometry coincides with the one showed in Figure 1 and the system size was 12800 × 50 × 1 nm^3 with periodic boundary condition in y-direction. To compare exactly with the analytical model, the calculations were performed without damping term and demagnetizing field. A domain wall was introduced at the center of the sample and then the system was excited with a monochromatic point source of 50 mT applied field, 1950 nm away from the domain wall. The amplitudes were calculated comparing the average envelope of the spin waves at both sides of the domain wall at the initial stages of the propagation. As D increases significant reflection is found for larger values of k. This is a direct result of the scattering terms in Equation (11).

As a result of the DMI, the scattering effective potential associated with the domain wall produces reflection in the spin waves propagating through it. Spin-wave reflection has been demonstrated due to the dipolar interaction in the absence of the DMI for propagation along the x- and y-directions.[31] In our model, spin waves propagating only along the x-direction are reflected, which makes it suitable for narrow nanowires. Spin-wave-driven domain wall motion has been explained in terms of linear momentum transfer.[32] When spin waves are reflected from the wall there is a linear momentum transfer. It has been shown that in the theoretical case when no damping is considered the linear momentum transfer leads to a rotation of the plane of the wall but not to domain wall motion.[31] We therefore expect that the inclusion of damping in our model would lead to a domain wall velocity, but the details are beyond the scope of this paper. It is important to emphasize that whatever physical mechanism is used to produce spin-wave reflection damping is a key ingredient for linear momentum transfer-domain wall motion.

To present the reflection in a clearer way and to highlight a consequence of the DMI for magnonics, we propose a periodic array of Bloch and Néel-type domain walls and calculate the band structure. For any wave propagating in a crystal, the Bragg reflection is the characteristic feature responsible for gaps at the edges of the first Brillouin zone, where the Bragg condition is satisfied. Similar to the ion cores in the nearly free electron model, in our case the periodicity of the crystal is determined by the periodic potential that describes the domain walls. In direct analogy to the scattering of electrons by a crystal, we Fourier transform Equation (21) and use the Bloch's theorem on $\chi(x)$ to obtain the central equation,

$$\left(Ak^2 - E\right)C(k) + \sum_G U_G C(k-G) = 0 \tag{25}$$

where U_G are the Fourier coefficients of the potential.[33] Equation (25) represents an infinite set of equations connecting the coefficients $C(k–G)$ for all reciprocal lattice vectors G. These equations are consistent if the determinant of the coefficients is zero. It is often only necessary to consider the determinant of a few coefficients. For our calculations an 11 × 11 matrix is used to numerically solve the central equation.

The period of the Dzyaloshinskii domain wall crystal can be determined with the Kooy–Enz formula that describes the stray field energy for an arrangement of parallel band domains separated by domain walls of zero width.[34] For a particular case of D = 2.6 mJ m^{-2} and a film thickness of 2 nm, the period is found to be L = 100 nm. The order of magnitude of the calculated period agrees with previous experimental results obtained in a system of two monolayers of iron on top of tungsten where the magnetic period was found to be 50 ± 5 nm.[27,35] We note also that this period depends on the magnitude of an external applied magnetic field, thus the periodicity can be adjusted with consequences on the band structure.

The calculated band structure of a domain wall crystal is shown in **Figure 4**. Our results are presented using the reduced zone scheme in which k is in the first zone, $-\pi/L \le k \le \pi/L$, and G is allowed to run over the appropriate reciprocal lattice points. The wave eigenfunctions at $k = \pm\pi/a$, where Bragg's condition is satisfied, are not traveling but standing waves

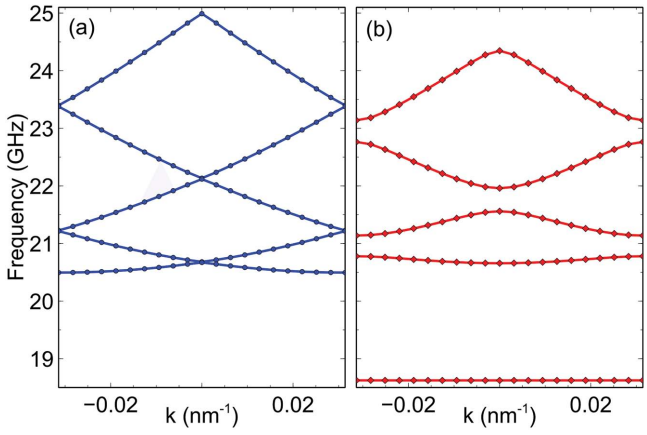

Figure 4. Calculated band structures of a domain wall crystal. No gaps at the edges of the Brillouin zone are found when the domain walls forming the periodic array are of a) the Bloch-type. In contrast, b) shows the band structure of a periodic array of Dzyaloshinskii domain walls where gaps of different magnitudes determined by the strength of the DMI (D = 1.56 mJ m^{-2}) are found at the edges of the Brillouin zone.

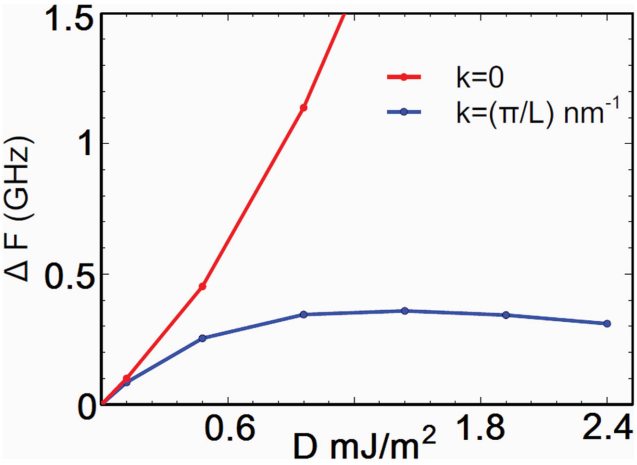

Figure 5. Frequency gaps ΔF at the Brillouin zone boundary as a function of D_c. $L = 100$ nm^{-1} is the period of the crystal.

formed by incident and reflected contributions. The origin of the gap can be understood by considering the probability densities. For a pure traveling wave, $\psi = \exp(ikx)$, its probability density is $\rho = |\psi|^2 = 1$, which is independent of the space coordinate and therefore of k. In contrast, for standing waves, $\psi_s \approx \sin(\pi x/L)$, the probability density, $\rho = |\psi_s|^2 \propto \sin^2(\pi x/L)$, vanishes for $x = L$, which corresponds to the center of the potential and to $\pm\pi/a$ in k space producing gaps. When the periodic array consists of Bloch-type walls (Figure 4a) there is no reflected contribution and the spin-wave traveling modes, $\chi_k(x)$ (Equation (8), do not produce gaps. However, the DMI favors the formation of Néel-type walls (Figure 4b) that reflect the spin waves described by the hybridized mode, $\chi(x)$ (Equation (17), causing the gaps in the band structure. Note that the translational invariance prevents the formation of a band structure for propagation along the y axis.

Figure 5 shows the first gap frequencies as a function of $D < D_{c2}$ in $k = 0$ and $k = \pi/L$. For $k = 0$, the gap frequency increases monotonically for the values of D considered, while for $k = \pi/L$ the gap reaches a maximum which for the parameters used in this work is $\Delta F \approx 0.5$ GHz.

5. Conclusion

We have discussed the effects of the interface form of the DMI on spin waves propagating perpendicular to the plane of a DMI-driven Néel domain wall. Unlike the common nonreciprocal dispersion found in other systems with DMI, we find a frequency shift as compared to the dispersion found in the Bloch-type walls. We calculate the spin-wave eigenstate and find that the localized mode hybridizes with the traveling modes as a result of an extra chiral term in the effective potential that describes the domain wall. While in the Bloch-type walls, spin waves are not reflected and only acquire a phase shift, we find that the DMI term in the effective potential scatters the spin waves and leads to reflection. We propose a periodic array of domain walls to highlight the reflection phenomenon. The band structure of the array exhibits gaps that resemble the ones found in magnonic crystals. An advantage of our proposed model over magnonic crystals based on nanostructures with alternating magnetic parameters relies in the fact that an external, applied magnetic field can be adjusted to modify the width of the domains suggesting the possibility of a tunable device. Acoustic and optical bands, and control over the frequency gaps are immediate consequences of such a tunable crystal. Another advantage of our model comes from the fact that domain walls are natural elements that minimize the energy of a magnetic system and therefore would at least ease some nanofabrication issues. Nevertheless, we recognize that the stabilization of the domains would be rather difficult because of magnetostatic effects, treated here within a local approximation, that would prevent straight and planar walls to be formed. Narrow nanowires might relieve this problem. Moreover, spin-wave damping is expected to be enhanced due to the spin–orbit origin of the DMI. While for the gaps in the band structure our proposal may still find applications in samples with relatively weak DMI with consequently small band gaps, another phenomenon may be enhanced: spin-wave-driven domain wall motion due to linear momentum transfer is known to depend linearly on the damping.

Acknowledgements

This work was partially supported by the University of Glasgow, EPSRC (EPSRC EP/M024423/1.,[36] the National Council of Science and Technology of Mexico (CONACyT), and the French National Research Agency (ANR) under contract no. ANR-11-BS10-003 (NanoSWITI).

Received: June 30, 2015
Revised: October 3, 2015
Published online: December 16, 2015

[1] I. Dzyaloshinsky, *J. Phys. Chem. Solids* **1958**, *4*, 241.
[2] T. Moriya, *Phys. Rev.* **1960**, *120*, 91.
[3] T. Moriya, *Phys. Rev. Lett.* **1960**, *4*, 228.
[4] A. Fert, V. Cros, J. Sampaio, *Nat. Nano* **2013**, *8*, 152.
[5] S. Rohart, A. Thiaville, *Phys. Rev. B* **2013**, *88*, 184422.
[6] A. Brataas, *Nat. Nanotechnol.* **2013**, *8*, 485.
[7] A. Thiaville, S. Rohart, É. Jué, V. Cros, A. Fert, *EPL Europhys. Lett.* **2012**, *100*, 57002.
[8] J.-P. Tetienne, T. Hingant, L. J. Martínez, S. Rohart, A. Thiaville, L. H. Diez, K. Garcia, J.-P. Adam, J.-V. Kim, J.-F. Roch, I. M. Miron, G. Gaudin, L. Vila, B. Ocker, D. Ravelosona, V. Jacques, *Nat. Commun.* **2015**, *6*, 6733.
[9] K. Zakeri, Y. Zhang, J. Prokop, T.-H. Chuang, N. Sakr, W. X. Tang, J. Kirschner, *Phys. Rev. Lett.* **2010**, *104*, 137203.
[10] L. Udvardi, L. Szunyogh, *Phys. Rev. Lett.* **2009**, *102*, 207204.
[11] J.-H. Moon, S.-M. Seo, K.-J. Lee, K.-W. Kim, J. Ryu, H.-W. Lee, R. D. McMichael, M. D. Stiles, *Phys. Rev. B* **2013**, *88*, 184404.
[12] D. Cortés-Ortuño, P. Landeros, *J. Phys.: Condens. Matter* **2013**, *25*, 156001.
[13] F. Garcia-Sanchez, P. Borys, A. Vansteenkiste, J.-V. Kim, R. L. Stamps, *Phys. Rev. B* **2014**, *89*, 224408.
[14] F. Garcia-Sanchez, P. Borys, R. Soucaille, J.-P. Adam, R. L. Stamps, J.-V. Kim, *Phys. Rev. Lett.* **2015**, *114*, 247206.
[15] J. M. Winter, *Phys. Rev.* **1961**, *124*, 452.

[16] H.-B. Braun, *Phys. Rev. B* **1994**, *50*, 16485.
[17] C. Bayer, H. Schultheiss, B. Hillebrands, R. L. Stamps, presented at *Magn. Conf. 2005 INTERMAG Asia 2005 Dig. IEEE Int.* Nagoya, Japan, **2005**, pp. 827.
[18] A. N. Bogdanov, U. K. Rößler, *Phys. Rev. Lett.* **2001**, *87*, 037203.
[19] Y. Le Maho, J.-V. Kim, G. Tatara, *Phys. Rev. B* **2009**, *79*, 174404.
[20] J. Lekner, *Am. J. Phys.* **2007**, *75*, 1151.
[21] A. A. Thiele, *Phys. Rev. B* **1973**, *7*, 391.
[22] J. Kishine, A. S. Ovchinnikov, *Phys. Lett. A* **2011**, *375*, 1824.
[23] A. Hubert, R. Schäfer, *Magnetic Domains: The Analysis of Magnetic Microstructures,* Springer, Berlin, Heidelberg **2008**.
[24] A. Hubert, *Phys. Status Solidi B* **1969**, *32*, 519.
[25] K.-S. Ryu, L. Thomas, S.-H. Yang, S. Parkin, *Nat. Nanotechnol.* **2013**, *8*, 527.
[26] S. Emori, U. Bauer, S.-M. Ahn, E. Martinez, G. S. D. Beach, *Nat. Mater.* **2013**, *12*, 611.
[27] M. Heide, G. Bihlmayer, S. Blügel, *Phys. Rev. B* **2008**, *78*, 140403.
[28] R. Hertel, W. Wulfhekel, J. Kirschner, *Phys. Rev. Lett.* **2004**, *93*, 257202.
[29] S. Flugge, *Practical Quantum Mechanics*, Vol. *1*, Springer, Berlin **1971**.
[30] A. Vansteenkiste, J. Leliaert, M. Dvornik, M. Helsen, F. Garcia-Sanchez, B. V. Waeyenberge, *AIP Adv.* **2014**, *4*, 107133.
[31] P. Yan, A. Kamra, Y. Cao, G. E. W. Bauer, *Phys. Rev. B* **2013**, *88*, 144413.
[32] P. Yan, X. S. Wang, X. R. Wang, *Phys. Rev. Lett.* **2011**, *107*, 177207.
[33] C. Kittel, *Introduction to Solid State Physics*, Wiley, New Jersey **2004**, p. 162.
[34] C. Kooy, U. Enz, D. Loss, *Philips Res. Rep.* **1960**, *15*, 7.
[35] A. Kubetzka, M. Bode, O. Pietzsch, R. Wiesendanger, *Phys. Rev. Lett.* **2002**, *88*, 057201.
[36] P. Borys, F. Garcia-Sanchez, J.-V. Kim, R. L. Stamps, DOI: 10.5525/gla.researchdata.196

